JOURNAL OF AIRCRAFT
Vol. 39, No. 1, January–February 2002

Experimental Investigation of Self-Actuating, Upper-Surface, High-Lift-Enhancing Effectors

Götz Bramesfeld* and Mark D. Maughmer†
Pennsylvania State University, University Park, Pennsylvania 16802

The increase in the maximum lift of an airfoil caused by small, movable tabs mounted on its upper surface has been explored in low-speed, wind-tunnel experiments at a chord Reynolds number of 1.0×10^6. These devices, herein called lift-enhancing effectors, have a chord that is 9% that of the airfoil and deploy passively at angles of attack approaching stall. Compared to the clean airfoil, the maximum lift coefficient is increased by approximately 20% with these simple devices. The lift increase is mainly caused by the effectors acting as "pressure dams," allowing lower pressures upstream of their location than would occur otherwise. At an effector the pressure recovers in a stepwise manner and continues downstream toward a trailing-edge value that is higher than that of the clean airfoil. This higher trailing-edge pressure also contributes to the increase in lift by allowing higher pressures over much of the lower surface. It has been shown that, in the absence of separation, properly installed effectors will lay flush on the surface and allow the airfoil to have the same performance in the low-drag range as the clean airfoil.

Introduction

MEASUREMENTS using the 14.4% thick HQ-41 airfoil on which narrow spanwise strips were attached on the aft portion of the upper surface showed, in comparison to the baseline airfoil, a 10–25% increase in the maximum lift coefficient.[1] In these experiments the chordwise width of each strip was 10% of the airfoil chord, and they were hinged at their leading edges to the airfoil. Similar devices, herein called lift-enhancing effectors (LEEs), are depicted in Fig. 1. These devices deploy passively under the influence of separated flow progressing toward the leading edge as the angle of attack increases. The amount of deployment is governed mainly by the pressures that occur over the airfoil. In Ref. 1 it is assumed that it is the momentum of the reversed flow that causes the effectors to deploy. In describing how these lift-enhancing devices operate, an analogy is made to the cover feathers of bird wings, which stand up during landing and appear to aid separation control in the high-lift regime. The enhancement of the high-lift region can be achieved without an undesirable impact on the low-drag region of the airfoil by making the effectors lie flush with the surface in the absence of flow separation.[1] Additional experiments using the 12.3% thick HQ-35 airfoil showed comparable gains in maximum lift coefficients, and it was again demonstrated that such gains can be achieved without penalties in the low-drag operating range of the airfoil.[2]

Although directed toward a very different application, data from wind-tunnel tests on spoilers and dive brakes also corroborate the lift-increasing potential of the upper-surface effectors. Spoilers and dive brakes increase overall aircraft drag by increasing profile drag and by "spoiling" the wing lift distribution such that higher induced drag results. Of particular relevance are measurements made on the 17% thick FX-67-VC-170 airfoil equipped with a 10% chord spoiler located at 80% chord.[3] As these measurements were directed toward obtaining data for spoiler applications rather than for lift augmentation, the angles of spoiler deployment were fixed at 30 and 90 deg. Nevertheless, a relative increase in the maximum lift coefficient of approximately 15% was measured. Measurements made on airfoils having scissors-type (Schempp–Hirth) dive brakes show similar results.[3]

The temporary availability of a pressure-orifice-equipped model in the Pennsylvania State University wind tunnel afforded the opportunity to explore the performance of the lift-enhancing effectors using surface pressure and wake survey measurements. In addition to allowing verification of the results obtained in other facilities, the surface-pressure distribution data allow insight into the functioning of the effectors that is not possible with the force-balance and wall pressure integration methods used in the studies noted.[1–3]

Experimental Procedure

Wind Tunnel

The experiments reported herein were conducted in the Pennsylvania State University Low-Speed, Low-Turbulence Wind Tunnel. This facility is a closed-throat, single-return, atmospheric tunnel with a test section measuring 1.0×1.5 m. Numerically controlled turntables are used to set the angle of attack of the two-dimensional model. The turntables are flush with the floor and ceiling of the tunnel and rotate with the vertically mounted model. At a velocity of 46 m/s, the flow angularity is below ± 0.25 deg everywhere in the test section. At the same velocity the mean velocity variation in the test section is below $\pm 0.2\%$, and the turbulence intensity is less than 0.045% (Refs. 4 and 5). The Pennsylvania State University wind tunnel is equipped with a numerically controlled traversing probe that automatically aligns with the local flow direction as the angle of attack changes. For these tests the nose of the probe was positioned 0.7 chords downstream of the model trailing edge.

Model

The model used in these experiments was of the 17.7% thick S824 airfoil, shown in Fig. 1, which was designed for use on vertical-axis wind turbines.[6] Although the design is symmetrical, a small amount of asymmetry was introduced during the manufacturing process. The chord length of the model is 45.6 cm. The upper and lower surfaces each have 30 pressure orifices. These orifices are 0.8 mm in diameter and drilled normal to the local surface. Although the relatively low maximum lift coefficient of 0.89 makes the S824 less than ideal for investigations of high lift, it was chosen for these experiments mainly because of its availability. In addition, a large amount of data for the clean airfoil without lift-enhancing effectors is available from earlier measurements and thus provides a baseline for comparison.[6]

The lift-enhancing effectors are made of 0.35-mm-thick Mylar tape extending over the complete span of the model. The chordwise

Received 8 December 2000; revision received 15 August 2001; accepted for publication 20 August 2001.

*Graduate Lecturer, Department of Aerospace Engineering. Student Member AIAA.

†Professor, Department of Aerospace Engineering, 229 Hammond Building. Senior Member AIAA.

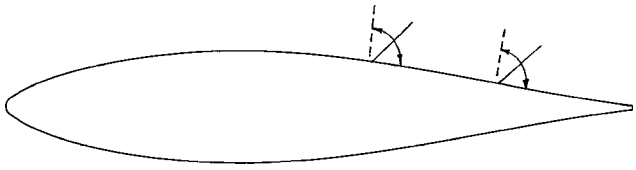

Fig. 1 S824 airfoil shown with self-actuated upper-surface high-lift augmentation effectors.

width of the effectors is approximately 4.0 cm or about 9% of the model chord. The devices were attached at their leading edges to the model upper surface using tape that also acted as a hinge with reasonably low stiffness. The chordwise location of the effectors is referenced to this attachment point. The effectors were restricted from deploying beyond 90 deg with respect to the local airfoil surface.

Tests

In the experiments discussed here surface-pressure distributions and wake survey measurements were obtained. Each pressure value was averaged from 500 samples that were taken at 500 Hz. The surface pressures were reduced to standard pressure coefficients and integrated to obtain sectional lift and pressure drag coefficients, as well as pitching-moment coefficients about the quarter-chord point. Section profile drag coefficients were obtained from the wake total and static pressures using standard procedures.[7] Standard low-speed, wind-tunnel wall corrections have been applied to all of the coefficients presented.[8] The data were obtained with free transition at a chord Reynolds number of 1.0×10^6.

The uncertainty of a measured force coefficient depends on the operating condition and generally increases with increasing angles of attack.[9] In the higher lift regions, with which the experiments that are discussed herein are mostly concerned, the measured lift coefficients have an uncertainty of $\Delta c_l = \pm 0.005$. Because no pressure orifices were located on the effectors, the lift coefficients presented do not account for the force contribution caused by the pressure differences between the front and backsides on the effectors themselves. An estimate using the surface-pressure differential across the effector locations, however, demonstrates that this contribution is insignificant. In the high-lift region the drag coefficients have an uncertainty of $\Delta c_d = \pm 0.00015$.

Flow visualization using fluorescent oil was used to detect transition locations and regions of separated flow.[10] It was also used to verify the two-dimensionality of the flow throughout these experiments.

Measurements were taken on several configurations in which one or two effectors were mounted at different chord locations. The first configuration tested had a single effector mounted with its leading edge at 86% chord. The choice for this location was based on the results of the predicted boundary-layer behavior for the airfoil, as well as on the observations described in Ref. 1. In particular, the theoretical analysis shows a small separated region aft of 95% chord that remains relatively stationary over much of the low-drag region of the airfoil. Once the angle of attack exceeds the upper limit of the low-drag region, i.e., $\alpha > 7$ deg, the separation point starts moving forward. Reference 1 describes that the effector is pushed up by the reversed flow. Thus, by mounting the effector so that its trailing edge is at 95% chord, it is upstream of the small separated region until the angle of attack is greater than that of the upper limit of the low-drag range.

In addition to the single effector at 86% chord, measurements were made with a single effector at 55% chord, with double effectors at 55 and 86% chord and with double effectors at 70 and 86% chord.

Experimental Results

The lift and moment curves for the baseline airfoil, along with those for a single effector at 86% chord and for double effectors at 70 and 86% chord, are presented in Fig. 2, whereas the corresponding drag polars are given in Fig. 3. In comparing these results, the increase in the maximum lift coefficient achieved by the effectors is of the most significance. For both the single- and double-effector

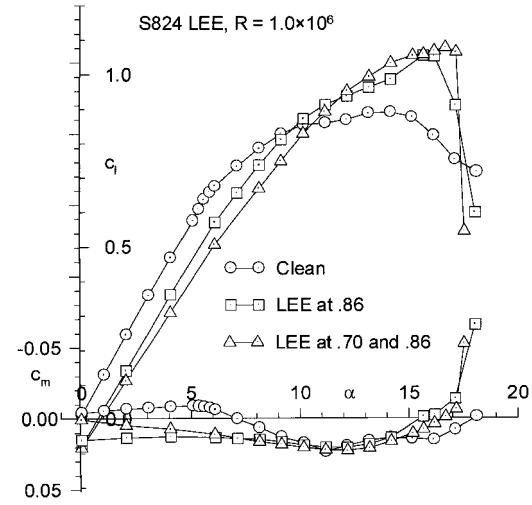

Fig. 2 Lift and moment coefficients vs angle-of-attack curves of the baseline S824 airfoil along with those of single and double effector-equipped configurations.

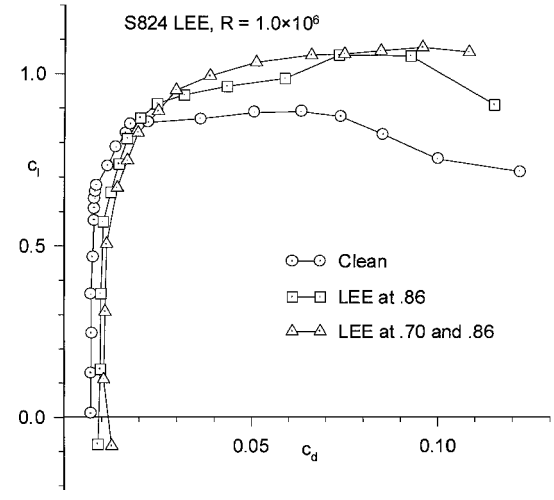

Fig. 3 Lift vs drag coefficient curves of the baseline S824 airfoil along with those of single- and double-effector-equipped configurations.

configurations the maximum lift coefficient is increased over that of the clean airfoil by approximately 18–20%.

In addition to the beneficial lift increase, it is observed that the drag in the low-drag range is increased, and the effectors cause the zero-lift angle of attack and pitching moment to be shifted in the positive direction. These are consequences of the effectors not being "nested" properly and, thus, being slightly deployed throughout the low-drag region in these experiments. In an actual application this would not be the case.

Single Effector at 86% Chord

As shown in Fig. 2, the configuration with a single effector hinged at 86% chord achieves lift coefficients that exceed those of the clean airfoil as soon as the effector begins to deploy. This occurs at an angle of attack of about 9 deg. The effector is fully deployed, normal to the local airfoil surface, at $\alpha = 14$ deg. There is a noticeable increase in lift curve slope as the angle of attack is increased further. The maximum lift coefficient of 1.05 is reached at $\alpha = 16$ deg, which is significantly more than the clean airfoil value of 0.89 at $\alpha = 14$ deg.

Fluorescent oil-flow studies on the clean airfoil show that at $\alpha = 14$ deg, the turbulent separation point is at about 42% chord. With an effector at 86% chord, the separation point moves aft to about 48% chord, and no explicit reversed-flow pattern is observable aft of the effector. On the upstream facing side of the effector, a stagnation point is indicated at the middle of the surface, and from

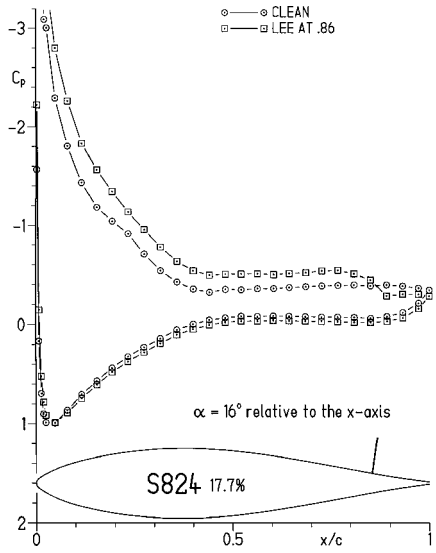

Fig. 4 Pressure distributions for $\alpha = 16$ deg of baseline S824 airfoil and of configuration having a single effector at 86% chord.

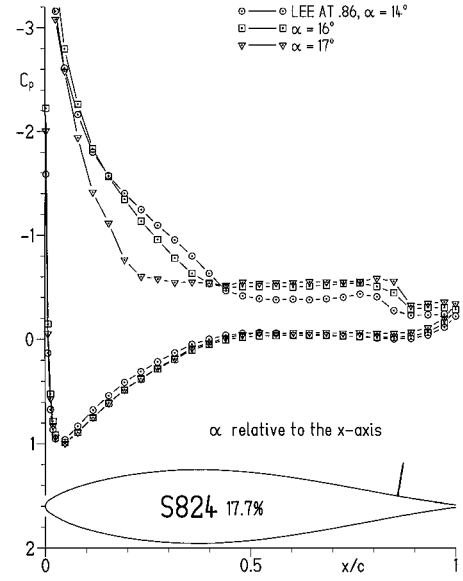

Fig. 5 Pressure distributions with one effector at 86% chord for several angles of attack.

there oil is transported to leading and trailing edges of the effector. This marks the presence of a recirculation region at the base of the effector. With and without effectors a laminar separation bubble, which is about 1% of the chord length, is visible near the leading edge of the airfoil. No significant three-dimensional effects are observed at this angle of attack with either configuration.

The pressure distributions measured at an angle of attack of 16 deg for the clean airfoil and for that having a single effector at 86% chord are presented in Fig. 4. In comparing these results, the most noticeable difference is a pressure recovery step occurring at the effector location. Upstream of that point, the pressures on the effector-equipped airfoil reach lower values than those on the clean airfoil. The leading-edge suction peak is not shown in this plot, or in any subsequent ones, to allow for a scale that better illustrates the pressure differences in the vicinity of the effectors. The upper-surface suction peak of the effector-equipped airfoil reaches a value of $C_p = -6.97$, whereas that of the clean airfoil is $C_p = -5.54$. The pressures downstream of the effector are higher than those occurring at corresponding locations on the clean airfoil. Because of the higher pressure at the trailing edge, the effector version also supports a higher pressure over the entire lower surface. In addition to producing the higher suction peaks, flow visualization studies show that the flow is attached approximately 10% further downstream on the effector-equipped airfoil than it is on the clean one. Based on the measured pressure distributions, it is estimated that of the total 28% increase in lift at this angle of attack about 85% comes from the decreased pressures on the upper surface, with the balance caused by the increased pressures on the lower surface.

Pressure distributions for angles of attack from $\alpha = 14$ to 17 deg for the configuration with a single effector at 86% chord are presented in Fig. 5. For these angles of attack, all of the pressure distributions exhibit upstream separated flow, followed by a pressure recovery step across the effector, followed by another separated region up to the trailing edge. Just upstream of the pressure rise is a small favorable gradient from about 70 to 80% chord, which becomes slightly less favorable as the angle of attack increases. This favorable pressure gradient is an indication of recirculating flow upstream of the effector. As the angle of attack is increased from 14 deg to that at which the airfoil stalls, 16 deg, the separation point moves upstream from about 55% to about 42% chord. As the angle of attack is increased beyond stall to 17 deg, the separation point moves forward to about 25% chord. The separation points on the clean airfoil that correspond to the same angles of attack, respectively, are at 42, 40, and 22% chord. Again, the corresponding suction peaks are not shown in that Fig. 5, but the measured pressure coefficients are -5.87, -6.97, and -6.73, respectively, for the three angles of attack.

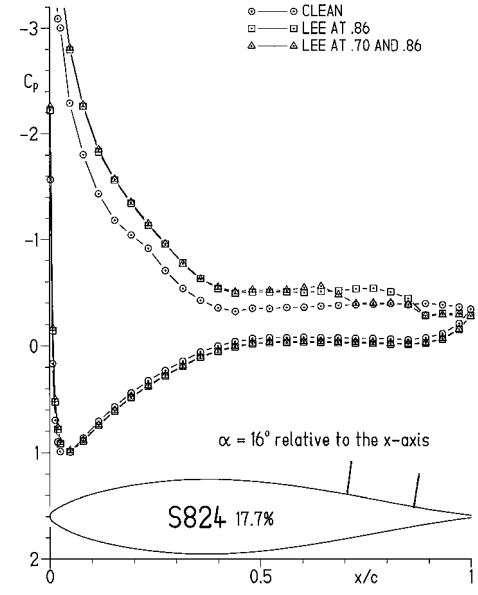

Fig. 6 Pressure distributions for $\alpha = 16$ deg of baseline S824 airfoil and of configurations having a single effector at 86% and double effectors at 70 and 86%.

Effectors at 70 and 86% Chord

As shown in Fig. 2, the configuration with effectors at 70 and 86% chord has a lift-curve behavior that is similar to that of the single effector. As soon as the angle of attack increases beyond that corresponding to the upper limit of the low-drag region, the deployment angle of the aft effector increases until, at an angle of attack of 14 deg, it is deployed fully. As this occurs, the upstream effector is deployed at an angle of about 30 deg with respect to the local airfoil surface. Both effectors are fully deployed when the maximum lift coefficient of 1.08 is reached. This value is only slightly greater than that obtained with the single effector, although it is achieved without the increase in lift-curve slope that occurs in the case of the single-effector-equipped airfoil. As is the case with the single effector, the lift decreases very abruptly when the angle of attack is increased beyond that of stall.

The pressure distributions shown in Fig. 6 are for the clean airfoil, for the airfoil having a single effector at 86% chord, and for the double-effector configuration with devices at 70 and 86% chord. The double-effector version achieves essentially the same overall

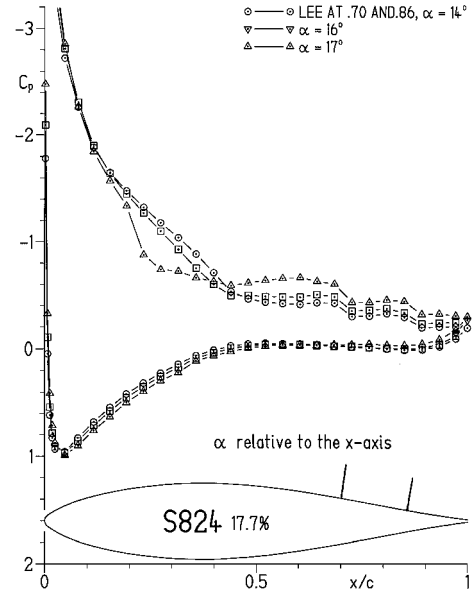

Fig. 7 Pressure distributions with effectors at 70 and 86% for several angles of attack.

integrated results as the single-effector configuration, but has pressure levels between the two effectors that are the same as those of the clean airfoil and pressures behind the second effector that are the same as those of the single-effector version. From the pressure distributions it appears that the flow is separated aft of 45% chord, as well as in the region between the effectors. The leading-edge suction peak of the double-effector-equipped airfoil $C_p = -7.25$, is lower than that of the single-effector configuration $C_p = -6.97$, and of the clean airfoil $C_p = -5.54$.

Pressure distributions for angles of attack from $\alpha = 14$ through 17 deg are plotted for the double-effector configuration in Fig. 7. On the upper surface a large pressure recovery step occurs across each effector. As with the single effector, a small favorable gradient exists just upstream of each effector and is most obvious in front of the effector at 70% chord. The pressure distribution shown for $\alpha = 17$ deg is immediately poststall. The leading-edge suction peaks for the angles of attack presented in the figure have pressure coefficients of -6.12, -7.25, and -7.61, corresponding to increasing angles of attack of 14, 16, and 17 deg.

Discussion

Lift

The results presented herein corroborate those of Refs. 1 and 2, namely, that effectors on the upper surface of an airfoil increase the maximum lift coefficient by about 20%. The lift increase is mainly caused by a reduction in the upper-surface pressures that occur upstream of the effectors. The pressure recovery that occurs across a deployed effector raises the pressure at the trailing edge to a value that is slightly greater than that of the clean airfoil. Thus, the effector can be regarded as a "pressure dam," across which the upstream and downstream pressures are decoupled. In addition to the reduced pressures on the upper surface in front of the effector, the slightly higher pressures over the entire lower surface contribute roughly 15% to the total increase in lift.

In general, separated flow regions and their lower pressures contribute to the production of lift by rear loading the upper surface of an airfoil; however, this also has a detrimental effect on the overall lift by reducing the leading-edge suction peak. Near stall, the suction peak collapses under the influence of the separation point having moved forward. This change from front to aft loading on the airfoil is often reflected in an increase in nose-down pitching moment near and beyond maximum lift. Furthermore, as the pressure in the separated region remains essentially constant to the trailing edge, this influences the lower surface-pressure distribution by lowering it and further contributing to the loss in lift. In the presence of a deployed effector, the pressure of the rearward separation is less able to propagate upstream. Until the thickness of separation exceeds the height of the fully deployed effector, a difference in pressures upstream and downstream of the effector can exist. As a result, the upstream pressures, including those of the leading-edge suction peak, are significantly lower than those in the separated region near the trailing edge.

Overall, it is found that the more forward an effector is located, the lower the pressures upstream of it will be. The resulting gains in lift expected as a result of these lower pressures, however, are offset because this more forward location of the effector reduces the extent of surface over which these lower pressures act. The maximum lift coefficient that can be achieved is the result of this tradeoff. Based on the experiments discussed herein, the largest gains in maximum lift occur when the effectors are located fairly far aft. It is also noted from the results presented, as well as others,[2] that the sharpness of the stall can be softened by a more forward placement of an effector.

Drag

The drag coefficients of the clean airfoil and two effector-equipped configurations are plotted against lift coefficient in Fig. 3. As has already been noted, within the low-drag range the effector-equipped airfoils have greater drag than the clean airfoil and have, as well, their zero-lift angles of attack and moments shifted in the positive direction. This is because the effectors in these experiments are not nested as they would be in an actual application and, consequently, are slightly deployed even at low angles of attack. As demonstrated in Refs. 1 and 2, it is possible to avoid the premature deployment in the absence of separation by using an effector with porosity or with a jagged trailing edge so that sufficient pressure relief is provided. Because the focus of the experiments reported here is on the nonlinear portion of the lift curve, when the deployment of the effectors is intended in order to augment the maximum lift, investigations with porous effectors were not performed.

As shown in Fig. 3, at lift coefficients above 0.85 the effector-equipped configurations show considerably better performance than does the clean airfoil. For example, at the angle of attack of the maximum lift coefficient of the clean airfoil $\alpha = 14$ deg, the single-effector version has nearly 15% less drag and produces about 10% more lift than the clean airfoil.

Conclusions

The augmentation of the maximum lift coefficient of an airfoil by about 20% from upper-surface, high-lift effectors was explored experimentally in the Pennsylvania State University Low-Speed, Low-Turbulence Wind Tunnel. The results obtained using surface-pressure integration are in close agreement with the force-balance measurements of other researchers.[1,2] Further corroboration of such an increase is provided by the results obtained using wall-pressure integration on an airfoil having a deployed spoiler.[3] Thus, three different measurement methods strongly support the validity of the measured increase in maximum lift coefficient.

The effectors deploy passively as the forward boundary of separated flow moves upstream with increasing angles of attack. From the surface-pressure distributions it is apparent that the effectors act as pressure dams that reduce the adverse effects of the separation on the pressure distribution of the attached flow upstream.

The results of the experiments presented herein suggest that further research on these devices is warranted. Additional work is necessary to get a better understanding of the influence of the location, length, and deployment angle of the effector on the maximum lift. In addition, the behavior of the effectors in three-dimensional, as well as unsteady flow, should be examined more closely.

Acknowledgments

The contributions of Jennifer Hansen, who assisted during the wind-tunnel tests discussed in this paper, are gratefully acknowledged. In addition, the authors would like to acknowledge the many valuable suggestions and efforts of the reviewers.

References

[1]Bechert, D. W., Bruse, M., Hage, W., and Meyer, R., "Biological Surfaces and Their Application—Laboratory and Flight Experiments on Drag Reduction and Separation Control," AIAA Paper 97-1960, June–July 1997.

[2]Schlobach, S., "Experimente zur Strömungsbeeinflussung Mittels Rückstromklappen und Wirbelgeneratoren am Laminarprofil HQ-35," Studienarbeit, Technical Univ. Berlin, Germany, Dec. 1999.

[3]Althaus, D., and Wortmann, F. X., *Stuttgarter Profilkatalog I*, Vieweg and Sohn, Braunschweig, Germany, 1981, pp. 204–212.

[4]Brophy, C. M., "Turbulence Management and Flow Qualification of The Pennsylvania State University Low Turbulence, Low Speed, Closed Circuit Wind Tunnel," M.S. Thesis, Dept. of Aerospace Engineering, Penn State Univ., University Park, PA, Dec. 1993.

[5]Medina, R., "Validation of The Pennsylvania State University Low-Speed, Low-Turbulence Wind Tunnel Using Measurements of the S805 Airfoil," M.S. Thesis, Dept. of Aerospace Engineering, Penn State Univ., University Park, PA, Dec. 1994.

[6]Maughmer, M. D., "Wind-Tunnel Test of the S824 Airfoil," National Renewable Energy Lab., Golden, CO., Rept. XAM-6-15504-01, July 1999.

[7]Prankhurst, R. C., and Holder, D. W., *Wind-Tunnel Technique*, Sir Isaac Pitman and Sons, Ltd., London, 1965, pp. 274–283.

[8]Allen, H. J., and Vincenti, W. G., "Wall Interference in a Two-Dimensional-Flow Wind Tunnel, with Consideration of the Effect of Compressibility," NACA Report 782, 1944.

[9]Kline, S. J., and McClintock, F. A., "Describing Uncertainties in Single-Sample Experiments," *Mechanical Engineering*, Vol. 75, No. 1, 1953, pp. 3–8.

[10]Loving, D. L., and Katzoff, S., "The Fluorescent-Oil Film Method and Other Techniques for Boundary-Layer Flow Visualization," NASA Memo 3-17-59L, 1959.